Available online at www.sciencedirect.com

ScienceDirect

Mendeleev Commun., 2021, **31**, 24–26

Mendeleev Communications

Composite nanoparticles with titania–poly(*N*-vinylamide) core–shell structure

Galina M. Kuz'micheva,[a] Olesya I. Timaeva,*[b] Irina P. Chikhacheva,[a] Roman V. Svetogorov,[b] Ratibor G. Chumakov,[b] Natalia V. Sadovskaya,[c] Pavel V. Dorovatovskii[b] and Raisa P. Terekhova[d]

[a] *MIREA – Russian Technological University, 119571 Moscow, Russian Federation*
[b] *National Research Center 'Kurchatov Institute', 123182 Moscow, Russian Federation. E-mail: olesyatimaeva19@gmail.com*
[c] *A. V. Shubnikov Institute of Crystallography, Russian Academy of Sciences, 119333 Moscow, Russian Federation*
[d] *A. V. Vishnevsky Institute of Surgery, 117997 Moscow, Russian Federation*

DOI: 10.1016/j.mencom.2021.01.006

Composite nanoparticles with a core consisting of associated anatase crystallites and a polymeric shell consisting of poly(*N*-vinylpyrrolidone) or poly(*N*-vinylcaprolactam) were synthesized and found to have antimicrobial activity against *Escherichia coli* and *Staphylococcus aureus* as well as photocatalytic activity in decomposition of methyl orange and methylene blue dyes. The highest antibacterial activity of the particles with poly(*N*-vinylpyrrolidone) shell is due to the larger amount of SO_4^{2-} groups and water adsorbed on the surface, while their photocatalytic activity is comparable with that of commercial nano-anatase samples.

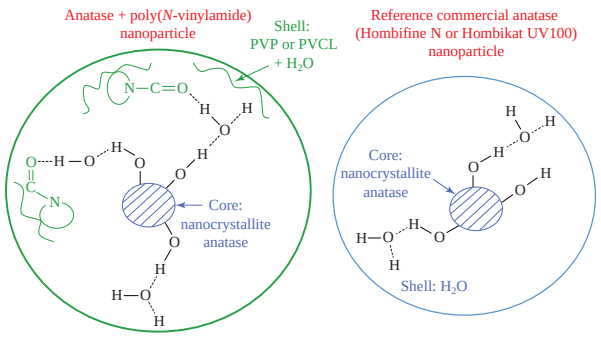

Keywords: nanoparticles, titania, anatase, polymers, photocatalysis, antimicrobial activity.

Core–shell nanoparticles are characterized by promising physicochemical properties, polyfunctionality as well as the possibility to optimize the target properties of their core and shell. Titania nanoparticles are known to have a broad spectrum of photocatalytic activity against microorganisms[1] and find an application as a catalyst for organic synthesis in medicinal chemistry,[2] while TiO_2–polymer nanomaterials are environmentally friendly and retain the antimicrobial action.[3] Thus, Desussa P25 TiO_2–polypropylene nanocomposites, where Degussa P25 TiO_2 represented a mixture of ~80% anatase and ~20% rutile, demonstrated toxicity to *Escherichia coli* under UV irradiation,[4] while a correlation was found between the methylene blue (MB) photodegradation and the inactivation of *E. coli* O157:H7 strain by the nanocomposite films of cellulose acetate and Degussa P25 TiO_2.[5] Low-density polyethylene films containing a mixture of anatase and rutile TiO_2 revealed the antimicrobial effect against *Pseudomonas spp.* and *Rhodotorula mucilaginosa* under UV irradiation as well.[6] Chitosan films containing TiO_2 nanoparticles effectively inhibited the growth of *E. coli*, *Staphylococcus aureus*, *Candida albicans* and *Aspergillus niger* under visible irradiation, with full sterilization after 12 h.[7] Photocatalytic properties of TiO_2 nanoparticles and bactericidal activity of chitosan were synergistically combined in their composites having visible radiation-induced antimicrobial activity for *E. coli*, *S. aureus* and *A. niger*.[8] For the antimicrobial nanocomposites, it is important that their disinfection effect could be achieved with no release of potentially toxic nanoparticles into the surrounding media.[9,10] As polymeric components of the composites, poly(*N*-vinylpyrrolidone) (PVP) and poly(*N*-vinylcaprolactam) (PVCL) can be considered as biocompatible and low toxic ones.[11,12] Anatase TiO_2–PVCL core–shell nanoparticles were synthesized and characterized in our work,[13] their core consisted of either single nanoparticles of the nanosized anatase or their associates.

In this work, core–shell nanoparticles were prepared from nano-TiO_2 and high-molecular-weight PVP (sample 1) or PVCL (sample 2) using the hydrothermal sulfate method from titanyl sulfate hydrate $TiOSO_4 \cdot x H_2O$ (for the details of synthesis, characterization as well as photocatalytic and antimicrobial tests, see Online Supplementary Materials). Hombikat UV100 and Hombifine N as the known commercial nano-anatase particles were synthesized by sol–gel and sulfate methods, respectively, and used as reference samples.

Samples 1 and 2 consisted of nano-anatase as the main phase as well as an amorphous hydrated phase of the $TiO_{2-x}(OH)_{2x} \cdot y H_2O$ composition[14] and/or $(TiO)(HSO_4)_x(OH)_y$ phase, the last sulfur-containing component was absent in the reference nano-anatase samples (Figure 1, Tables S1 and S2, see Online Supplementary Materials). The amorphous hydrated TiO_2 phase was present in all the samples due to their synthesis conditions, though to a lesser extent in sample 1 (Figure S1, peak with $2\theta \sim 10$–$12°$, see Online Supplementary Materials). It is known that these amorphous phases are formed in the shell of anatase nanoparticles under powerful synchrotron irradiation.[13] The known reflections of PVP and PVCL,[15] namely peaks with $2\theta \sim 9$ and 18°,[13] were absent in the X-ray diffraction patterns of all samples (Figures 1 and S1), however, the presence of the polymers in samples 1 and 2 was confirmed by IR spectroscopy, XPS and CHNS element analysis (Figures S2–S4, Table S2).

The refinement of the nano-anatase crystalline structure in samples 1 and 2 by the Rietveld method (Table S1) revealed a greater amount of vacancies (□) in the titanium site for sample 1

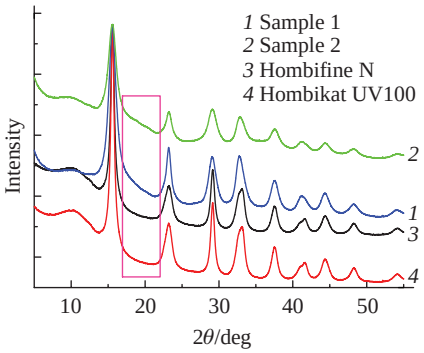

Figure 1 X-ray diffraction patterns of the samples synthesized compared with the reference commercial nano-anatase particles, the background difference region is indicated by a rectangle.

($Ti_{0.923(14)}\square_{0.077}O_2$) compared with the Hombifine N ($Ti_{0.966(8)}\square_{0.034}O_2$)[13] and Hombikat UV100 ($Ti_{0.968(8)}\square_{0.032}O_2$) references. An increase in the vacancy concentration with a decrease in the average crystallite sizes was observed. Sample 1 had the smallest average crystallite size and the least microstrains content (Table S1). According to XPS data, the number of oxygen vacancies on the surface of nanoparticles decreases in the following order: sample 2 (24.3%) > Hombikat UV100 (24%) > sample 1 (9.8%) > Hombifine N (7.7%) (Figure S4).

As follows from SEM images, samples 1 and 2 have different microstructure (Figure S5) with nanoparticles size in the range from ~10–30 to >100 nm. The presence of a small number of coarse particle associates larger than 100 nm is characteristic of both samples.

Then, antimicrobial activity of the nanoparticles was tested. The reference nano-anatase samples had no effect in the dark against *S. aureus*, *E. coli* and *C. albicans* (Figure 2).

Samples 1 and 2 revealed the growth delay zone >10 mm for *E. coli* and *S. aureus* but did not demonstrate activity against the fungi. The best effect for sample 1 is presumably associated with the larger content of sulfur in the form of SO_4^{2-} on the particles surface along with physically adsorbed water. Samples 1 and 2 with antimicrobial activity in the dark can be employed for further design of biocidal nanomaterials, for example, in wastewater treatment[16] and preparation of antimicrobial agents.[17]

The assessment of photocatalytic activity of the nanoparticles for the degradation of methyl orange (MO) dye revealed greater effect for the reference nano-anatase samples (Figure 3), although sample 1 approached the Hombifine N activity. Under irradiation of a 26 W UV lamp, an increase in the temperature of the dye solution up to 33 °C was detected, however, at this temperature the phase transition of PVCL did not occur yet, *i.e.*, the core–shell structure was preserved. Hombikat UV100 had larger photocatalytic activity in the MO decomposition compared with Hombifine N due to the larger specific surface and oxygen

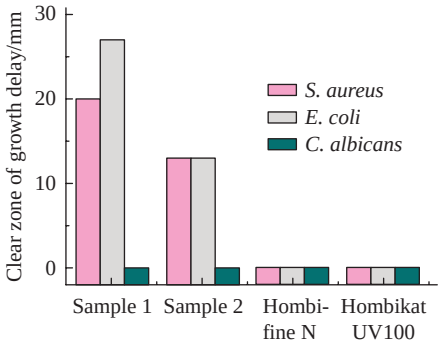

Figure 2 The antimicrobial activity of the synthesized and reference nanoparticles.

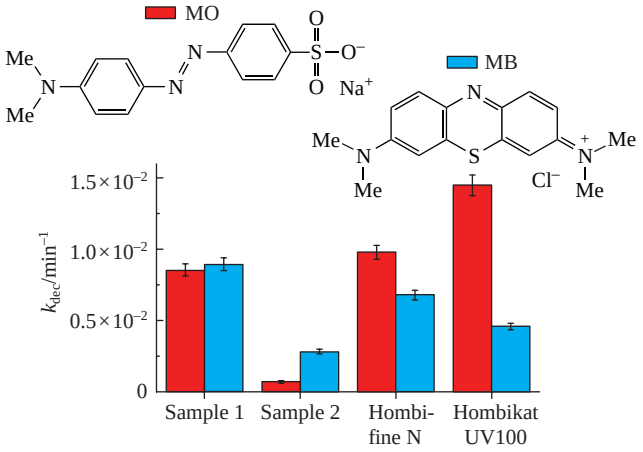

Figure 3 Rate constants for photodecomposition of MO and MB dyes catalyzed by the synthesized and reference nanoparticles.

vacancy content on the surface of the former nanoparticles,[18] while other characteristics of the reference nano-anatase samples were almost identical (Table S1). Sample 1 had better photocatalytic activity in the MB dye degradation compared with other nanoparticles (see Figure 3). Its advantage over sample 2 is due to smaller crystallite sizes as well as the absence of oxygen vacancies in the titania bulk and on the nanoparticles surface (Table S1), which favors the recombination of charge carriers as an important factor for photocatalytic activity.

In summary, composite nanoparticles with a core consisting of associated anatase crystallites and a polymeric shell consisting of PVP or PVCL were synthesized and found to have antimicrobial activity against *E. coli* and *S. aureus* as well as photocatalytic activity in decomposition of MO and MB dyes. The highest antibacterial activity of the particles with PVP shell is due to the larger amount of SO_4^{2-} groups and water adsorbed on the surface, while their photocatalytic activity is comparable with that of commercial nano-anatase samples. Since the commercial Hombifine N and Hombikat UV100 references have demonstrated promising results in photodegradation of pesticides and fungicides,[19] the investigated TiO_2–PVCL and TiO_2–PVP core–shell nanoparticles can find application in this area as well as may be employed as a basis for the development of new antimicrobial agents.

This work was supported by the Ministry of Science and Higher Education of the Russian Federation (grant no. 0706-2020-0026).

Online Supplementary Materials

Supplementary data associated with this article can be found in the online version at doi: 10.1016/j.mencom.2021.01.006.

References

1 S. Josset, N. Keller, M.-C. Lett, M. J. Ledoux and V. Keller, *Chem. Soc. Rev.*, 2008, **37**, 744.
2 A. A. Rempel and A. A. Valeeva, *Russ. Chem. Bull., Int. Ed.*, 2019, **68**, 2163 (*Izv. Akad. Nauk, Ser. Khim.*, 2019, 2163).
3 A. Kubacka, M. S. Diez, D. Rojo, R. Bargiela, S. Ciordia, I. Zapico, J. P. Albar, C. Barbas, V. A. P. Martins dos Santos, M. Fernández-Garcia and M. Ferrer, *Sci. Rep.*, 2014, **4**, 4134.
4 T. Huppmann, S. Yatsenko, S. Leonhardt, E. Krampe, I. Radovanovic, M. Bastian and E. Wintermantel, *AIP Conf. Proc.*, 2014, **1593**, 440.
5 J. Xie and Y.-C. Hung, *LWT–Food Sci. Technol.*, 2018, **96**, 307.
6 H. Bodaghi, Y. Mostofi, A. Oromiehie, Z. Zamani, B. Ghanbarzadeh, C. Costa, A. Conte and M. A. Del Nobile, *LWT–Food Sci. Technol.*, 2013, **50**, 702.
7 X. Zhang, G. Xiao, Y. Wang, Y. Zhao, H. Su and T. Tan, *Carbohydr. Polym.*, 2017, **169**, 101.

8 T. Qian, H. Su and T. Tan, *J. Photochem. Photobiol., A*, 2011, **218**, 130.
9 A. Kubacka, C. Serrano, M. Ferrer, H. Lünsdorf, P. Bielecki, M. L. Cerrada, M. Fernández-Garcia and M. Fernández-Garcia, *Nano Lett.*, 2007, **7**, 2529.
10 V. AshaRani, G. L. K. Mun, M. P. Hande and S. Valiyaveettil, *ACS Nano*, 2009, **3**, 279.
11 S. V. Jadhav, D. S. Nikam, V. M. Khot, N. D. Thorat, M. R. Phadatare, R. S. Ningthoujam, A. B. Salunkhe and S. H. Pawar, *New J. Chem.*, 2013, **37**, 3121.
12 Yu. E. Kirsh, *Prog. Polym. Sci.*, 1993, **18**, 519.
13 O. Timaeva, V. Nikolaichik, R. Svetogorov and G. Kuz'micheva, *Z. Kristallogr. – Cryst. Mater.*, 2020, **235**, doi: 10.1515/zkri-2019-0051.
14 M. Dadachov, *US Patent Application 2006/0171877 A1*, 2006.
15 O. Timaeva, I. Chihacheva, G. Kuzmicheva, N. Ivanovskaya and A. Dorohov, *J. Mater. Res.*, 2018, **33**, 1475.
16 A. Mathur, J. Kumari, A. Parashar, T. Lavanya, N. Chandrasekaran and A. Mukherjee, *PLOS One*, 2015, **10**, e0141301.
17 J. T. Seil and T. J. Webster, *Int. J. Nanomed.*, 2012, **7**, 2767.
18 P. A. Demina, A. M. Zybinskii, G. M. Kuz'micheva, L. N. Obolenskaya, E. V. Savinkina and N. A. Prokudina, *Crystallogr. Rep.*, 2014, **59**, 430 (*Kristallografiya*, 2014, **59**, 477).
19 S. P. Mulakov, P. M. Gotovtsev, A. A. Gainanova, G. V. Kravchenko, G. M. Kuz'micheva and V. V. Podbel'skii, *J. Photochem. Photobiol., A*, 2020, **393**, 112424.

Received: 15th July 2020; Com. 20/6264